 doi:10.20944/preprints201911.0155.v1

Article

Characterization of Cellulosic Cotton Residue Produced by Sanding Process and Applied to Cement Pastes

Mailon Lima [1,*], Julio Freitas [1], Caroliny Santos [2], Thiago Santos [2], Heriberto Oliveira [2,*] and Renata Braga [3]

[1] Chemistry department, Cement Laboratory; Federal University of Rio Grande do Norte, Av. Senador Salgado Filho, 3000, Lagoa Nova, 5907890, Natal/RN, Brazil; mailon.aguimar@gmail.com; juliofreitasj@hotmail.com

[2] Textile engineering department; Federal University of Rio Grande do Norte, Av. Senador Salgado Filho, 3000, Lagoa Nova, 5907890, Natal/RN, Brazil; carolinyminely@hotmail.com; heriberoliver@hotmail.com; thiagotextilufrn@hotmail.com

[3] Chemistry engineering department; Federal University of Rio Grande do Norte, Av. Senador Salgado Filho, 3000, Lagoa Nova, 5907890, Natal/RN, Brazil; renatabraga.r@gmail.com

* Correspondence: mailon.aguimar@gmail.com (M.L.); heriberoliver@hotmail.com or joseheriberto@ct.ufrn.br (H.O)

Abstract: Fiber-cement composites were prepared from cellulosic cotton residue (CCR) arise from sanding process (emerizing). The effect of different concentrations: 0.5% and 1%, and granulometry: thick (retained in a14 mesh sieve) and thin (retained in a 48 mesh sieve) of this residue were evaluated on tensile strength of cement slurries with seven (07) curing days. To characterize the CCR, TGA, FT-IR, SEM and XRD analysis were performed and the residue resistance in an alkaline environment was also evaluated. Splitting tensile strength test, known as Brazilian Test, was used to assess effects of the fibers on the mechanical behavior of cement matrix. Analyzing the results, the CCR proved to be resistant in an alkaline environment, meaning that it can withstand the alkaline environment of cement matrix. The results showed an improvement superior to 17% in tensile strength for 1% of CCR. Therefore, the CCR presents a great application potential in cement pastes used for oil well cementing that requires to increase its tensile strength, once a significant improvement was achieved with a low-residue employee.

Keywords: cellulosic cotton residual; sanding textile process; fiber-cement composites; tensile strength

1. Introduction

The fibers make up the yarn and several yarns make up the fabric. However, some fibers are not entirely contained in the yarn, so they end up exposed on the fabric surface, generating a visible and tactile appearance of unwanted roughness. To improve these aspects, the fabric is subjected to the sanding process.

Sanding is a mechanical process that consists of a surface wear made by cylinders covered by an abrasive material [1]. This process is performed after some previous treatment on fabric surface, including the mercerization. According to Babu et al. (2007), the mercerization consists in a treatment on textile fabric by a strong solution of sodium hydroxide and washing-off the caustic after 1 to 3 min, while holding the material under tension [2]. After the mercerizing process, non-cellulosic material (lignin, hemicellulose and waxes) are removed. So, the residue generated from sanding process is a cellulosic residue.

The textile industry produces large amounts of cellulosic cotton residue (CCR) at different stages of processing. These residues do not have defined use and cannot be used in animal nutrition due to chemicals used in the mercerization. However, the commercial value of this residue can be incremented through its use as reinforcement material in cement slurries, since this is a high-strength vegetable fiber.

The use of cellulosic fibers as reinforcement material in cementing slurries have been highlighted in literature due to its good mechanical properties, dimensional stability, low cost and biodegradability [3,4]. When the fibers are used in the proper amount and are homogeneously distributed, they reduce the fissures occurrence, increase the tensile strength, hardness, ductility, durability and improve other mechanical properties as well Bolat et al. 2014 and Ardanuy et al. 2011 [5,6].

Studies have been conducted in order to determine the effects of different cellulosic fibers addition in cement slurries used for civil construction [3,7–10]. Meanwhile, researches aimed to the application of these materials in oil wells cementing operations are limited.

According to Afroughsabet et al. (2016), the cement tensile strength is smaller than its compressive strength and, for this reason, the cracks propagate rapidly intension levels lower than the compressive tension levels. The tensile strength is the tractive force that the material could be subjected without a rupture. Slurries with a high tensile strength are extremely important to directional wells cementing, where there is a offset on the cementing angle that can reach 90°, conditioning themselves horizontally. Under these conditions, the paste is subjected to compressive forces on the top and traction forces on the bottom. A standard cement paste couldn't resist the traction generated in these conditions [11].

Therefore, in order to improve the tensile strength of cement slurries applied to oil well cementing, this study was focused to characterize the CCR generated from sanding process and evaluate the influence of different sizes and concentrations of this residue in the tensile strength of Special Class CPP cement slurries used in cementation operations of oil wells.

2. Materials and Methods

2.1. Materials

The cellulosic cotton residue (CCR) arise from the sanding process was acquired from a textile industry in Natal-RN, Brazil. The material was submitted to granulometric distribution, being selected the grains retained in sieves of 14 mesh (> 1.18 mm) and 48 mesh (> 0.297 mm).

2.2. Alkaline treatment

The CCR was subjected to alkaline treatment test according to the adapted standard ASTM D 6942-03, where 10 g of CCR was added into a solution of NaOH 1N, during a period of 1, 7, 14, 21 and 28 days, generating an alkalized cellulosic cotton residue (ACCR). The samples were washed until the pH close to 7 and submitted to analysis.

2.3. Experimental methods

2.3.1. Scanning electron microscopy (SEM)

The surface morphology of CCR, ACCR and the fiber-cement composites, were determined through micrographs obtained in the scanning electron microscope (SEM) from Philips® model EMEV LX 30. The samples were prepared through a thin gold layer deposition on the surface by sputter.

Preprints (www.preprints.org) | NOT PEER-REVIEWED | Posted: 14 November 2019 doi:10.20944/preprints201911.0155.v1

97 2.3.2. FT-IR spectroscopy
98
99 The chemical components of CCR and ACCR were studied through Fourier Transform Infrared
100 Spectroscopy (FT-IR) analysis, using the spectrophotometer IRAffinity-1, within the range of 4000 –
101 500 cm-1, with a resolution of 4 cm-1 and 32 scans.
102
103 2.3.3. Thermogravimetric analysis (TGA)
104
105 Thermogravimetric analysis of CCR and ACCR were conducted using a thermogravimetric
106 scale SDT Q600 from TA Instruments. The temperature range of 25 and 700°C was used, with a
107 heating rate of 10ºC/min under a state flow of 100mL/min N2 (99.99%).
108
109 2.3.4. X-ray diffraction
110
111 The X-ray diffraction profiles of CCR and ACCR were held in Eco D8 Advance from BRUKER,
112 using a Cu anode, at a voltage of 40 kV and current of 258 mA. Samples were scanned in 2θ with
113 scam ranging from 5° to 50°, with an increment of 0.03°. The identification of phases was performed
114 by the comparison between the peaks generated in diffractogram, using the program X'Pert
115 HighScore Plus standard charts. The crystallinity index of the cellulose was determined according to
116 the method of Segal et al. (1959), given by the equation [12]:
117
118

$$CI = 1 - \left(\frac{IAM}{I002}\right).100 \quad (1)$$

119
120
121 where: CI corresponds to the crystallinity index; IAM is the amorphous diffraction intensity; I_{002} =
122 maximum intensity of diffraction.
123
124 *2.4. Samples formulations and mixing*
125
126 The cement samples were formulated in accordance with the standards established by API RP
127 10B (American Petroleum Institute), with a specific gravity of 15.6 lb/gal, using Special Class Portland
128 cement and water, without chemical additives, to evaluate the fibers influence in the gain of
129 mechanical strength. The table 1 presents the nomenclature used in this work for the samples
130 formulated with CCR, raw residue, in sizes of 14 and 48 mesh and concentration of 0.5 and 1%.
131
132 A low content of CCR was used because above 1% the mixing would not be done properly.
133
134 *Table 1 Slurries formulation with specific gravity of 15.6 lb/gal*

Formulation	Cement (g)	Water (g)	CCR (g)
Standard	772,00	355,00	-
CCR-14-0.5	765,39	352,33	3,83
CCR-14-1	763,52	350,39	7,64
CCR-48-0.5	765, 39	352,33	3,83
CCR-48-1	763,52	350,39	7,64

135
136 The slurries preparation began with weighing the components according to the formulations
137 presented in Table 1. The mixture of solid components (cement and fiber residue), was performed
138 manually (dry mix), using a closed plastic container, stirring and mixing these components during 3
139 minutes.

The mixture was performed according to the procedures established by the API RP 10B, using a paste mixer 3060 from Chandler. The curing period of the slurries was carried out in a water bath during 7 days at 38 ºC.

2.5. Brazilian test

The cylindrical samples (Figure 1a) were ruptured according to the adapted standard NBR-722 (2010).

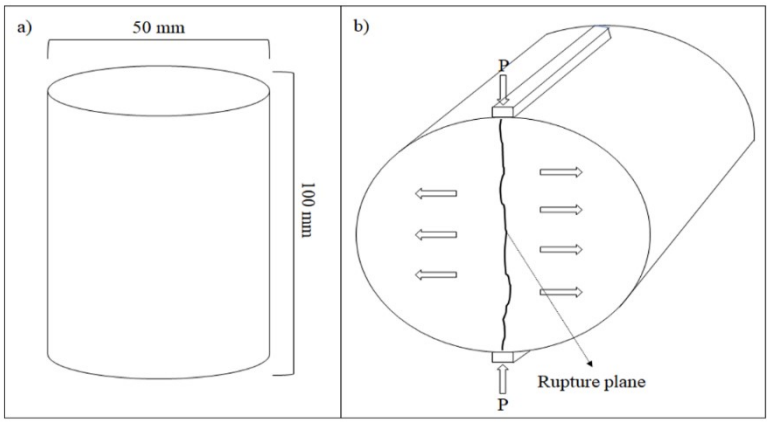

Figure 1 Brazilian test. a) Samples measure and b) schematic of Brazilian test.

The test consists in the application of a force (P) on a cylindrical specimen along two opposing sides (Figure1b), resulting in a relatively uniform tensile traction that acts on the vertical plane of the specimen, causing a rupture in the cylinder center. The tests were performed on a universal mechanical testing machine model Autograph AG-1 100 kN and data treatment by software Trapezium 2 from Shimadzu. A preload of 0,500N was initially applied, also a constant speed load of 17.9 MPa/min.

3. Results and Discussions

3.1. Scanning electron microscopy (SEM)

The Figure2 shows the morphology of the sample CCR and of the ACCR. The residues, raw and alkaline, presented tubular morphology and irregular diameter ranging from 5 to 20 μm. The CCR, Figs. 4a and 4a1, presented a rough aspect, that is characteristic of fibers that were subjected to a mercerization process. This roughness is the result from the impurities removal (waxes and oils), as well as removing most of the non-cellulosic components (lignin and hemicellulose) by alkaline treatment (Wang et al. 2016; Hendriks and Zeeman 2009), that is performed by the industry [13,14].

According to (Li et al. 2007), this post mercerizing roughness results in an increase of the fiber specific surface area, that leads to a greater adherence of this material to the cement matrix[15].

The samples subjected to the alkaline treatment for diferent number of days (ACCR01, ACCR 14 and ACCR 28, corresponding to 1, 14 and 28 days in alkaline solution), showed no signs of degradation after the treatment, but, a slight diminution on diameter for CCR and ACCR28, 15-20 μm and 5-18 μm respectively, means that a fraction of amorphous cellulose was removed from CCR during the alkaline treatment. According to Borchani et al. (2015), it may cause slight damage to the fiber structure and results in more exposed cellulosic fibrils [16]. This result is supported by the development of the crystallinity index of ACCRs, as shown in Table 2.

 doi:10.20944/preprints201911.0155.v1

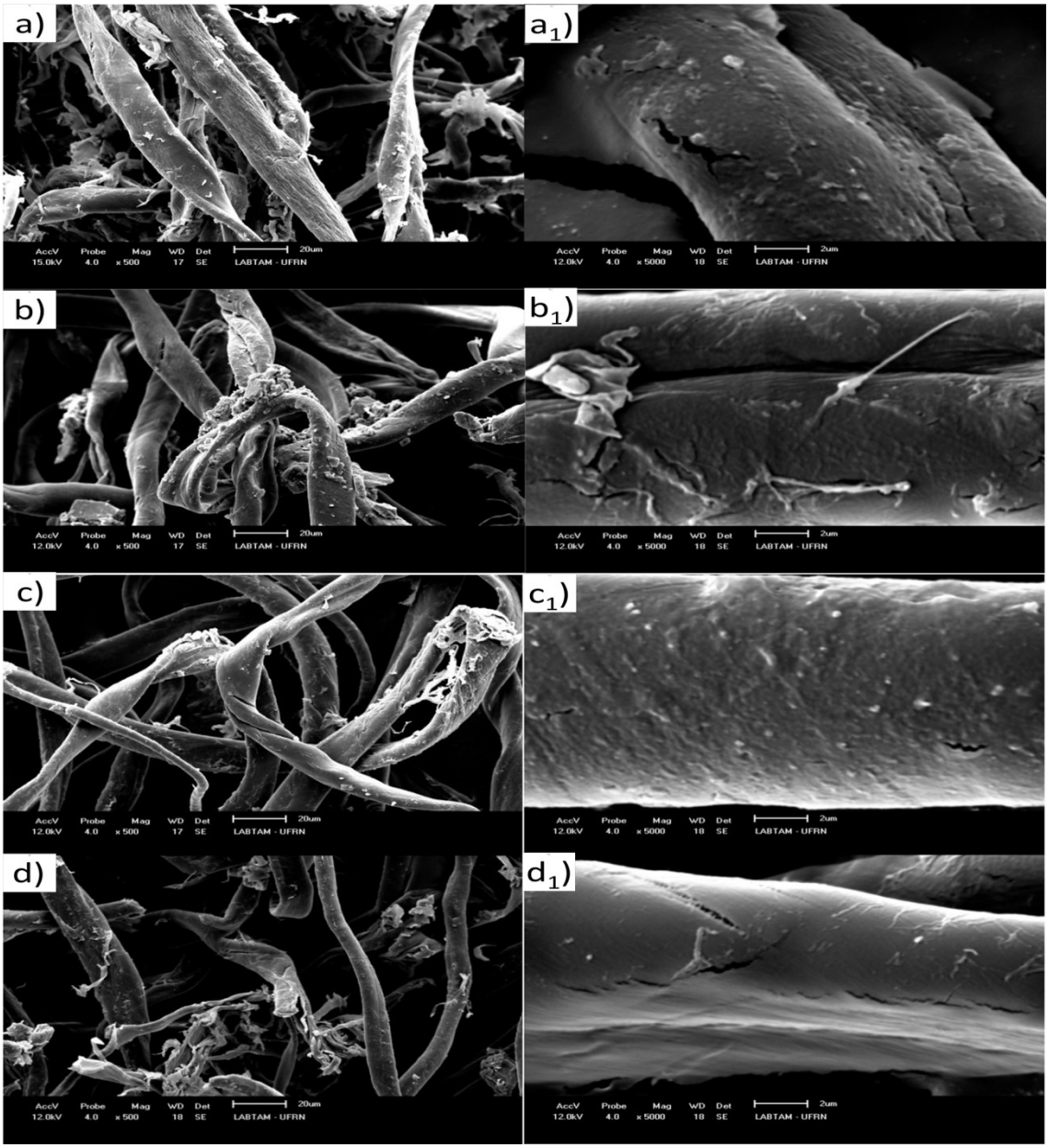

Figure 2 Surface morphology of CCR and ACCRs samples. a), a1) CCR; b), b1) ACCR01; c), c1) ACCR14 and d), d1) ACCR28

3.2. FT-IR analysis

Infrared spectra of CCR and ACCRs are presented in Figure3. In all spectra, the absorption bands correspond to common cellulosic absorption bands. The bands 3333 cm^{-1} and 1642 cm^{-1} corresponds to O-H stretching, from hydrogen bonding and adsorbed water respectively [17,18]. C-H stretches in 2920 cm^{-1} and 2850 cm^{-1} were also observed [17,19,20]. They were a little more intensive for ACCR07. Other characteristic bands are presented around 1028 cm^{-1}, corresponding to C-O alongation [21,22] and 894 cm^{-1}, which corresponds to stretching vibrations of C-O-C groups [16,22].

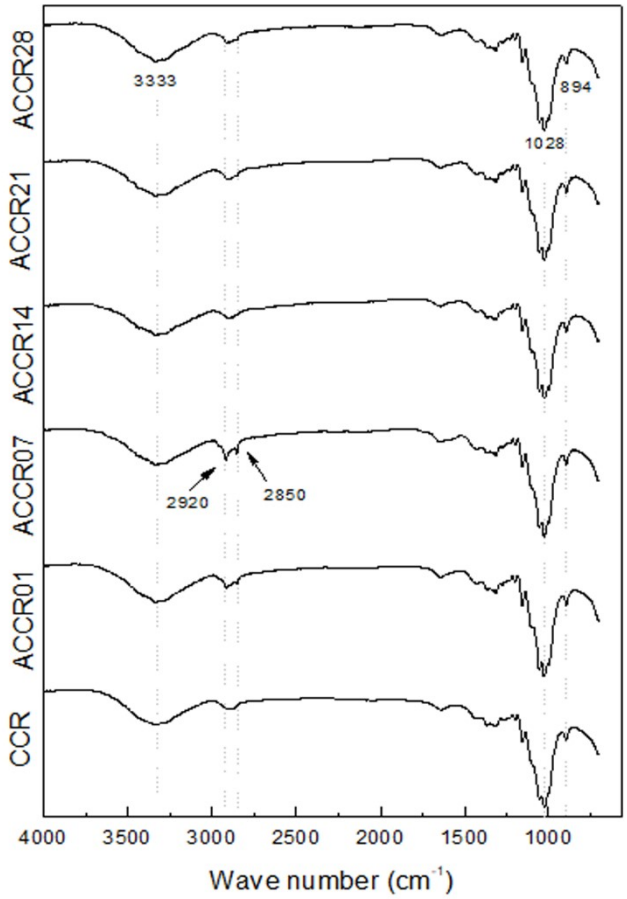

Figure 3 Infrared spectroscopy of CCR and ACCRs

It is possible to observe similar behavior among the specters presented in Figure1. This indicates no significant changes in the chemical structure of the residue exposed to to the alkaline environment. The work of Wang et al. (2016) also submitted cellulosic cotton residue to an alkaline treatment based on NaOH and NaOH/Urea, and also confirmed that no chemical reaction occurred during alkaline treatment [14,23,24].

3.3. TGA analysis

The thermogravimetric curves of the CCR and the ACCRs are presented in Figure4. It shows similar thermal decomposition profiles. Initially, in the first phase of pyrolysis, below 100 ºC, the mass loss was associated with the water vaporization. The second mass loss observed between 280-390 °C for the CCR and between 295-390° C for the ACCRs, is associated with the cellulose decomposition and, according to the literature, is degraded in a narrow temperature range due to homogeneous composition of glucose units in the cellulose [22,25]. ACCRs showed a light higher degradation temperature (295° C) than the CCR (280° C), which can be attributed to its greater crystallinity (Table 2)

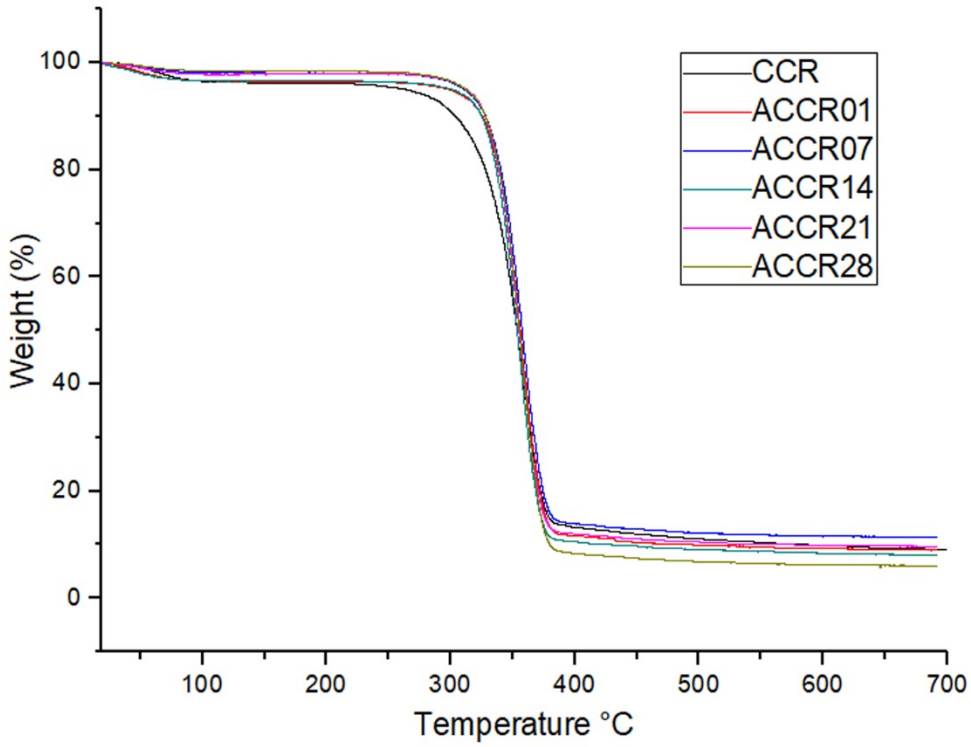

Figure 4 TGA of the CCR and ACCRs

The percentage of residual mass after heated at 700°C was 10.73% for the CCR and 6.17% for the ACCR28. This difference is associated with the solubilization of inorganic compounds during the alkali treatment, this result was confirmed through ash content test performed according to the ASTM E1755-01, where an ash content of 2.34% confirmed the presence of inorganic matter in CCR. Yeng et al. (2015) achieved a similar thermogravimetric curve working with commercial cellulose Avicel PH-101 [22]. Two mass losses were observed, the first one was associated with water evaporation and the second, between 300 and 360°C, was associated with the cellulose degradation. The residual mass was 13.92%.

Yu et al. (2017) used pure cotton cellulose obtained after treatment and observed that cellulose degradation occurred at the temperature ranging from 300 to 400 °C, with a residual mass of 5.5% at 700°C [25].

3.4. X-rain diffraction

The X-ray diffractograms, Figure5, shows peaks at 2θ = 15.08º ($1\bar{1}0$), 16.72º (110) and 22.56° (200), only confirming the presence of cellulose I in the residue. This result was already expected, once that the alkali treatment used in industry is done in low concentrations of NaOH. In studies developed by Yue et al. (2012), there was no conversion of Cellulose I into Cellulose II under a 10% NaOH treatment [26,27].

The cellulose crystallinity index (CI%) is presented in Table 2. Although it is non-exact, the method of Segal et al. (1959) is very useful in order to compare a specific behavior at a set of samples [12].

Table 2 Crystallinity index of CCR and the ACCRs

Sample	CCR	ACCR 01	ACCR 07	ACCR 12	ACCR 14	ACCR 28
Crystallinity index (%)	69.09	76.3	75.3	74.4	76.03	74.5

It can be noticed that the IC% of ACCRs are higher than the IC% from sample CCR, this increase was greater than 7.7%. According to Borchani et al. (2015), this result is associated with the alkaline treatment, that removed part of the fiber amorphous surface, resulting in an increase of the relative crystallinity [16]. Their studies, using a 1% alkaline treatment, presented an 12% increase in crystallinity of fibers Alpha Stem. The work of Ashori et al. (2012) was held in a 1% cotton fibers alkaline treatment, and achieved an 13% crystallinity increase [28].

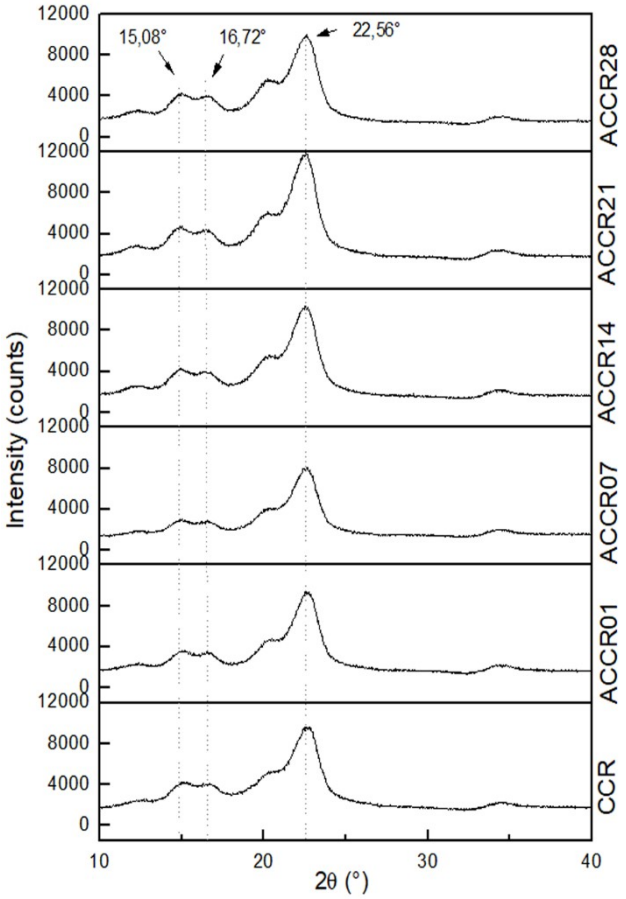

Figure 5 XRD analysis of the CCR and ACCRs

3.5. Brazilian test

The experimental methods used to characterize the fiber/matrix interaction, had been based on the composite final gain of mechanic resistance [29]. The most important mechanical tests for cement slurries are compression, tensile and bending resistance tests. The tensile resistance test is used to

 doi:10.20944/preprints201911.0155.v1

measure the forces that the material may be submitted before rupture. Pastes that have a high tensile strength are extremely important for directional wells cementing, a standard cement paste could not resist the traction generated in these conditions. Therefore, a solution for this problem would be the addition of natural fibers, that increases its tensile strength, hardness and impact resistance.

The results of the tensile strength of the standard (Portland cement + water) and fiber-cement composites (Portland cement + water + CCR) are presented in Figure6. It shows that the tensile strength increases is proportional to the concentration of residue used in the composition. Even with low levels of CCR, the formulations: CCR-14-1 and CCR-48-1 showed a gain of 17.1% and 20.43%, respectively, in the tensile strength values. This increase is because the fibers tend to cross through the fissures formed in the array, promoting a certain ductility after cracking. The higher the adherence of the fibers into the matrix, the more noticeable is this effect (Afroughsabet et al.2016) [11]. Kawashima and Shah (2011), obtained similar results by adding 1% of cellulosic fiber 100% raw (2.1 mm) into a regular class I Portland cement, the increase in tensile strength observed in their work was approximately 13.12% [30].

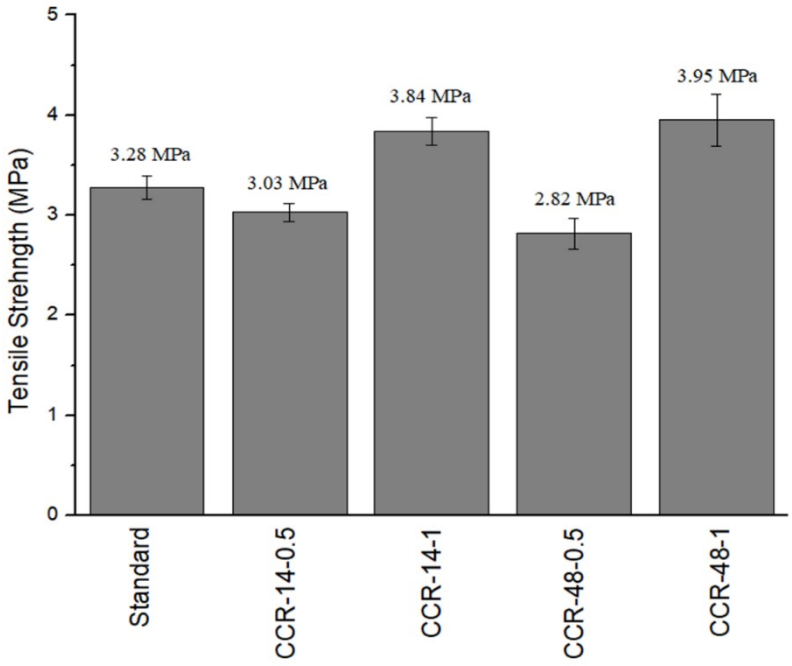

Figure 6 Mechanical tensile strength of the fiber-cement composites

Studies performed by Elsaid et al. (2011), evaluated the tensile strength gain in a regular Portland cement matrix, reinforced with Kraft cellulosic fiber (> 25 mm) [31]. The fiber content used was 2.4% and resulted in a tensile strength gain of 40%. This excessive gain can be associated with the higher fiber content used as reinforcement and also because it was no residue.

According to Mallick (1997), generally a high fiber content results in a greater tensile resistance gain [32]. However, there is a moment when a large amount of fiber inhibits an effective slurry homogenization, forming a cluster in the composite that decreases the mechanical properties. In this study, formulations containing more than 1% of fiber would inhibit the mixture of the pastes.

 doi:10.20944/preprints201911.0155.v1

In addition, analyzing Figure6, it is possible to observe that the tensile strength values suffered a small influence by the fiber size, when 1% of residue was used. There was a slightly tensile strength difference higher than 3% in the values of composites reinforced with 14 mesh (> 1.18 mm) and 48 mesh (> 0.297 mm) residues. According to Maher and Ho (1994); Silva et al. (2008), the smallest cellulosic material size tends to present best results of resistance gain [33,34]. It can be associated with the higher contact surface generated between fiber and matrix, as well as a better and more homogeneous fiber dispersion in the composite.

Both formulations containing 0.5% of CCR, CCR-14-0.5 and CCR-48-0.5, suffered a loss of 7.62% and 14% on their mechanical tensile strength respectively. In their study, Al-Oraimi and Seibi (1995) used 0.15% content of cellulosic fibers from palm leaves as reinforcement material in regular Portland cement matrix and obtained a reduction of 18.42% in the tensile strength value [35]. Jongvisuttisun and Kurts (2015) used a 0.5% content of wood cellulosic fiber in Portland cement matrix I/II, and after 7 and 28 days of curing the loss on tensile strength was 7.88% and 2.87%, respectively [36]. They assigned this loss with a common behavior of slurries with internal curing. However, the explanation given by Jongvisuttisun & Kurts (2015) does not apply to the 1% content, once that in this study and in the study of Kawashima and Shah (2011) there was an increase in tensile strength [30]. This result suggests that the effect of "bridge" produced by CCR is not effective in very low contents (0.5%), been necessary a minimum amount of fiber to hamper the fissures spread. This behavior was observed in the formulations containing 1% of fiber, where the increase of tensile strength indicates that tension was transferred from the array to the fibers[37].

3.6. FT-IR images of the samples

The images obtained by scanning electron microscopy analysis from three of five formulations are shown in Figure7. The CCR is easily identified.

The SEM analysis of the asbestos cement, fractured after 7 days of curing, and 13 more days until the tests, allowed to confirm the presence of the CCR with inorganic particles on its surface in the array, even after 20 days. This indicates that the residue can resist for a long period in cement matrix.

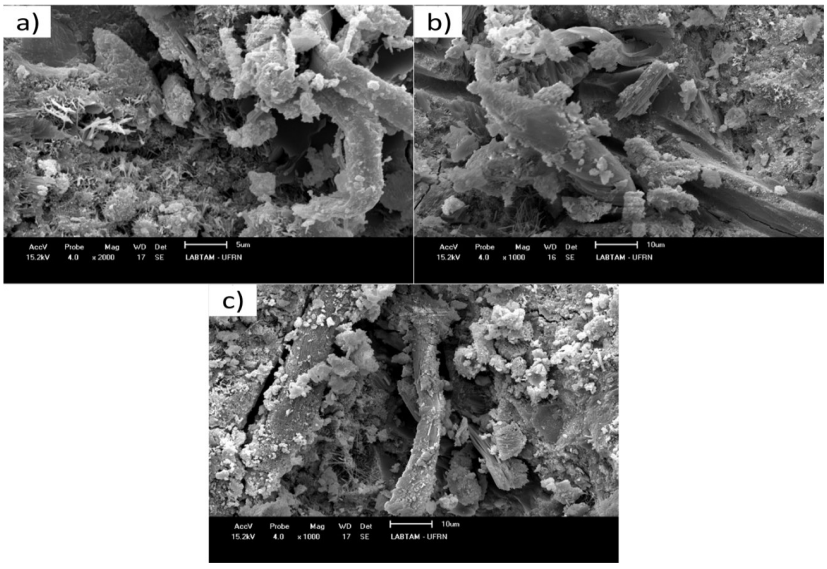

Figure 7 SEM images showing the interaction fiber/matrix a) C-14-0.5; b) C-48-0.5 e c) C-48-1

4. Conclusions

In this study, it was found that the CCR has a great potential to be used as a reinforcement material for oil well cementing slurries that require high tensile strength, once it seems resistant to alkaline environment. Other good point is that the industry performs mercerizing process on this residue which expand its surface area (as seem on SEM), enabling a better adhesion of this material to the cement matrix. However, it is necessary a minimum CCR (14 or 48 mesh) content, so they can mitigate the propagation of the fissures. Thus, a low concentration of residue (0.5%) resulted in tensile strength reduction, although, the samples containing 1% of CCR had an increment higher than 17% on its tensile strength. This was slightly more significant for the residue with smaller particle size, once that this residue held a greater dispersion and surface contact with the cement particles.

Author Contributions: The contribution of the authors of this manuscript was very important for its quality and goes far beyond: Freitas, J. C. O.; Braga, R. M. and Nascimento, J. H. O. conceived an idea of publication and supervision as a conclusion of this work. Lima, M. A. developed a theory, performed the experiment and the calculations. Freitas, J. C. O .; Braga, R. M. and Nascimento verified the analytical methods. All authors discussed the results and contributed to the final manuscript. Also, Braga, R. M. contributed to the preparation of the sample. Authors Santos, C. M. S and Santos, T. F. wrote the manuscript and contributed to a final version of the manuscript.

Funding: This research received no external funding.

Conflicts of Interest: The authors declare no conflict of interest.

References

1. Bueno, M.-A.; Lamy, B.; Renner, M.; Viallier-Raynard, P. Tribological investigation of textile fabrics. *Wear* **1996**, *195*, 192–200.
2. B. Ramesh Babu; A.K. Parande; S. Raghu, and T.P.K. An Overview of Wastes Produced During Cotton Textile Processing and Effluent Treatment Methods - Pesquisa Google. **2007**, 110–122.
3. Ballesteros, J.E.M.; dos Santos, V.; Mármol, G.; Frías, M.; Fiorelli, J. Potential of the hornification treatment on eucalyptus and pine fibers for fiber-cement applications. *Cellulose* **2017**, *24*, 2275–2286.
4. Matuana, L.M.; Balatinecz, J.J.; Sodhi, R.N.S.; Park, C.B. Surface characterization of esterified cellulosic fibers by XPS and FTIR spectroscopy. *Wood Sci. Technol.* **2001**, *35*, 191–201.
5. Ardanuy, M.; Claramunt, J.; García-Hortal, J.A.; Barra, M. Fiber-matrix interactions in cement mortar composites reinforced with cellulosic fibers. *Cellulose* **2011**, *18*, 281–289.
6. Bolat, H.; Şimşek, O.; Çullu, M.; Durmuş, G.; Can, Ö. The effects of macro synthetic fiber reinforcement use on physical and mechanical properties of concrete. *Compos. Part B Eng.* **2014**, *61*, 191–198.
7. Darsana, P.; Abraham, R.; Joseph, A.; Jasheela, A.; Binuraj, P.R.; Sarma, J. Development of Coir-fibre Cement Composite Roofing Tiles. *Procedia Technol.* **2016**, *24*, 169–178.
8. Ferreira, S.R.; Silva, F.D.A.; Lima, P.R.L.; Toledo Filho, R.D. Effect of fiber treatments on the sisal fiber properties and fiber-matrix bond in cement based systems. *Constr. Build. Mater.* **2015**, *101*, 730–740.
9. Tonoli, G.H.D.; Rodrigues Filho, U.P.; Savastano, H.; Bras, J.; Belgacem, M.N.; Rocco Lahr, F.A. Cellulose modified fibres in cement based composites. *Compos. Part A Appl. Sci. Manuf.* **2009**, *40*, 2046–2053.

10. Yadav, J.S.; Tiwari, S.K. Behaviour of cement stabilized treated coir fibre-reinforced clay-pond ash mixtures. *J. Build. Eng.* **2016**, *8*, 131–140.
11. Afroughsabet, V.; Biolzi, L.; Ozbakkaloglu, T. High-performance fiber-reinforced concrete: a review. *J. Mater. Sci.* 2016, *51*, 6517–6551.
12. Segal, L.; Creely, J.J.; Martin, A.E.; Conrad, C.M. An Empirical Method for Estimating the Degree of Crystallinity of Native Cellulose Using the X-Ray Diffractometer. *Text. Res. J.* **1959**, *29*, 786–794.
13. Hendriks, A.T.W.M.; Zeeman, G. Pretreatments to enhance the digestibility of lignocellulosic biomass. *Bioresour. Technol.* 2009, *100*, 10–18.
14. Wang, J.; Li, Y.; Wang, Z.; Li, Y.; Liu, N. Influence of pretreatment on properties of cotton fiber in aqueous NaOH/urea solution. *Cellulose* **2016**, *23*, 2173–2183.
15. Li, X.; Tabil, L.G.; Panigrahi, S. Chemical treatments of natural fiber for use in natural fiber-reinforced composites: A review. *J. Polym. Environ.* 2007, *15*, 25–33.
16. Borchani, K.E.; Carrot, C.; Jaziri, M. Untreated and alkali treated fibers from Alfa stem: effect of alkali treatment on structural, morphological and thermal features. *Cellulose* **2015**, *22*, 1577–1589.
17. Kale, R.D.; Bansal, P.S.; Gorade, V.G. Extraction of Microcrystalline Cellulose from Cotton Sliver and Its Comparison with Commercial Microcrystalline Cellulose. *J. Polym. Environ.* **2018**, *26*, 355–364.
18. Rojas, J.; Lopez, A.; Guisao, S.; Ortiz, C. Evaluation of several microcrystalline celluloses obtained from agricultural by-products. *J. Adv. Pharm. Technol. Res.* **2011**, *2*, 144.
19. Abidi, N.; Cabrales, L.; Haigler, C.H. Changes in the cell wall and cellulose content of developing cotton fibers investigated by FTIR spectroscopy. *Carbohydr. Polym.* **2014**, *100*, 9–16.
20. Uddin, M.J.; Cesano, F.; Scarano, D.; Bonino, F.; Agostini, G.; Spoto, G.; Bordiga, S.; Zecchina, A. Cotton textile fibres coated by Au/TiO2 films: Synthesis, characterization and self cleaning properties. *J. Photochem. Photobiol. A Chem.* **2008**, *199*, 64–72.
21. Chung, C.; Lee, M.; Choe, E.K. Characterization of cotton fabric scouring by FT-IR ATR spectroscopy. *Carbohydr. Polym.* **2004**, *58*, 417–420.
22. Yeng, L.C.; Wahit, M.U.; Othman, N. Thermal and flexural properties of regenerated cellulose(RC)/poly(3- hydroxybutyrate)(PHB)biocomposites. *J. Teknol.* **2015**, *75*, 107–112.
23. Cao, C.; Yang, Z.; Han, L.; Jiang, X.; Ji, G. Study on in situ analysis of cellulose, hemicelluloses and lignin distribution linked to tissue structure of crop stalk internodal transverse section based on FTIR microspectroscopic imaging. *Cellulose* **2015**, *22*, 139–149.
24. Lopes, F.F.M.; Araújo, G.T.; Luna, S.; Nascimento, J.W.B.; da Silva, V.R. Modificação das propriedades das fibras de curauá por acetilação. *Rev. Bras. Eng. Agric. e Ambient.* **2011**, *15*, 316–321.
25. Yu, Y.; Wang, J.; Wang, J.; Li, J.; Zhu, Y.; Li, X.; Song, X.; Ge, M. Highly fluorescent cotton fiber based on luminescent carbon nanoparticles via a two-step hydrothermal synthesis method. *Cellulose* **2017**, *24*, 1669–1677.
26. Kumar, A.; Negi, Y.S.; Choudhary, V.; Bhardwaj, N.K. Characterization of Cellulose Nanocrystals Produced by Acid-Hydrolysis from Sugarcane Bagasse as Agro-Waste. *J. Mater. Phys. Chem.* **2014**, *2*, 1–8.
27. Yue, Y.; Zhou, C.; French, A.D.; Xia, G.; Han, G.; Wang, Q.; Wu, Q. Comparative properties of cellulose nano-crystals from native and mercerized cotton fibers. *Cellulose* **2012**, *19*, 1173–1187.
28. Ashori, A.; Ornelas, M.; Sheshmani, S.; Cordeiro, N. Influence of mild alkaline treatment on the cellulosic surfaces active sites. *Carbohydr. Polym.* **2012**, *88*, 1293–1298.
29. Herrera-Franco, P.J.; Drzal, L.T. Comparison of methods for the measurement of fibre/matrix adhesion in composites. *Composites* **1992**, *23*, 2–27.

30. Kawashima, S.; Shah, S.P. Early-age autogenous and drying shrinkage behavior of cellulose fiber-reinforced cementitious materials. *Cem. Concr. Compos.* **2011**, *33*, 201–208.
31. Elsaid, A.; Dawood, M.; Seracino, R.; Bobko, C. Mechanical properties of kenaf fiber reinforced concrete. *Constr. Build. Mater.* **2011**, *25*, 1991–2001.
32. P.K. Mallick *Composites Engineering Handbook (Materials Engineering)*; 1997; ISBN 9780824793043.
33. Maher, M.H.; Ho, Y.C. Mechanical Properties of Kaolinite/Fiber Soil Composite. *J. Geotech. Eng.* **1994**, *120*, 1381–1393.
34. Silva, F. de A.; Chawla, N.; Filho, R.D. de T. Tensile behavior of high performance natural (sisal) fibers. *Compos. Sci. Technol.* **2008**, *68*, 3438–3443.
35. Al-Oraimi, S.K.; Seibi, A.C. Mechanical characterisation and impact behaviour of concrete reinforced with natural fibres. *Compos. Struct.* **1995**, *32*, 165–171.
36. Jongvisuttisun, P.; Kurtis, K.E. The role of hardwood pulp fibers in mitigation of early-age cracking. *Cem. Concr. Compos.* **2015**, *57*, 84–93.
37. Habel, K.; Viviani, M.; Denarié, E.; Brühwiler, E. Development of the mechanical properties of an Ultra-High Performance Fiber Reinforced Concrete (UHPFRC). *Cem. Concr. Res.* **2006**, *36*, 1362–1370.